Journal of the Optical Society of America A
OPTICS, IMAGE SCIENCE, AND VISION

Method to reduce undesired multiple fundus scattering effects in double-pass systems

Carlos E. García-Guerra,[1,2,*] Joan A. Martínez-Roda,[1] Mikel Aldaba,[1] Fernando Díaz-Doutón,[1] Meritxell Vilaseca,[1] Brian Vohnsen,[2] and Jaume Pujol[1]

[1]Centre for Sensors, Instruments and Systems Development (CD6), Universitat Politécnica de Catalunya (UPC), Rambla Sant Nebridi 10, Terrassa 08222, Spain
[2]University College Dublin (UCD), Advanced Optical Imaging Group (AOI), Dublin 4, Ireland
*Corresponding author: carlos.enrique.garcia@upc.edu

Received 17 October 2018; revised 5 March 2019; accepted 26 March 2019; posted 26 March 2019 (Doc. ID 348485); published 29 April 2019

Double-pass systems rely on backscattering of light by the human ocular fundus to assess the optical quality of the eye. In this work, we present a method to reduce double-pass image degradation caused by undesired multiple scattering effects in the eye fundus. The reduction is based on combined data processing of simultaneous measurements using two different configurations: one symmetric with equal entrance and exit pupils and another asymmetric with unequal entrance and exit pupils. Under certain conditions, such scattering effects may be effectively suppressed. Measurements of human eyes show that, although multiple fundus scattering imposes a shift on the estimations, double-pass systems can be used to predict the optical quality of the eye within a population.

https://doi.org/10.1364/JOSAA.36.000918

1. INTRODUCTION

The optical quality of the eye is estimated with the double-pass (DP) technique from the image of a point source projected onto the ocular fundus [1]. This surface is composed by the stratified layers of the sensory retina, including directional photoreceptors [2], the retinal pigment epithelium, Bruch's membrane, the choroid, and the sclera. Each of these structures has different absorption, reflection, and scattering properties [3,4]. At certain wavelengths, especially in the infrared region, light may penetrate up to the choroid, and diffuse laterally due to forward scattering by blood [5]. It is not clear if this multiple fundus scattering process can impact vision [6,7]. However, DP images may contain information about this particular diffuse reflectance that occurs in the fundus of the measured eye [8,9].

The contribution of multiple fundus scattering is perceived as a halo surrounding the central spot in DP images [10]. Such widening may affect the computation of parameters of relevance when determining the optical quality of the eye. For instance, the modulation transfer function (MTF) estimated with DP instruments is usually lower in magnitude than when computed using systems less directly affected by multiple scattering, such as interferometric devices [6] and Hartmann–Shack (HS) sensors [11], although these also capture average aberrations across the depth of the layered eye fundus. In this sense, a method to reduce the degradation caused by multiple scattering in the ocular fundus may improve the accuracy of optical quality estimators that rely on the DP technique.

The possibility of reducing blurring by multiple scattering effects in DP images has been discussed by different authors. López-Gil and Artal [10] proposed excluding the tails of the DP image below a certain threshold during the computation of the MTF. However, the region surrounding the DP spot contains information not only about fundus scattering, but also about intraocular scattering and ocular aberrations. García-Guerra *et al.* [12] estimated the response of fundus scattering based on the combined analysis of DP and HS data. Even so, the method was not used to either reduce or eliminate the influence of the fundus in DP estimations.

In this work, a method to reduce the impact of multiple fundus scattering in DP estimations is proposed. The procedure consists of recording a pair of images using an instrument that integrates two DP systems with a common first pass of light. The combination of entrance and exit pupil sizes forms a system based on a symmetric configuration with equal pupils, and another relies on an asymmetric arrangement with unequal pupils [13]. The proposed method removes the influence of the first pass of light in the asymmetric configuration using information from the arrangement with equal pupils. Under certain conditions, the undesired fundus scattering effects may be effectively suppressed by first determining their contribution from the symmetric DP image and later filtering them from the DP response with unequal pupils. The method has been tested using an artificial eye and applied to a total of 19 measurements in healthy human eyes.

2. METHODS

A. Reducing Broadening by Multiple Fundus Scattering in DP Data

The DP technique has been described mathematically previously [1,14]. A DP model where multiple scattering in the ocular fundus has been accounted for by multiplication in the Fourier domain has been presented before by us [12]. Assuming that such a model remains a valid approximation, suppose that two DP responses of the same eye under the following configurations are available: a first response for a symmetric system [14] with equal entrance and exit pupils of 2 mm in diameter ($\mathrm{MTF_{DPe}}$); and a second response for an asymmetric system [13] with unequal entrance and exit pupils of 2 and 4 mm in diameter ($\mathrm{MTF_{DPu}}$), respectively. The MTF for these configurations may be written as

$$\begin{aligned}\mathrm{MTF_{DPe}} &= \mathrm{MTF_{2\,mm}} \cdot \mathrm{MTF_{FS}} \cdot \mathrm{MTF_{2\,mm}}\\ \mathrm{MTF_{DPu}} &= \mathrm{MTF_{2\,mm}} \cdot \mathrm{MTF_{FS}} \cdot \mathrm{MTF_{4\,mm}},\end{aligned} \tag{1}$$

where $\mathrm{MTF_{FS}}$ accounts for the contribution of the multiple scattering that arises in the ocular fundus, and $\mathrm{MTF_{2\,mm}}$ and $\mathrm{MTF_{4\,mm}}$ represent the eye responses with exit pupils of 2 and 4 mm diameter, respectively, that contain also the effects of both aberrations and intraocular scattering.

The eye response with a 4 mm pupil is estimated with conventional data processing from the response $\mathrm{MTF_{DPu}}$ measured using the asymmetric DP configuration. In this estimation, the eye response $\mathrm{MTF_{2\,mm}}$ is considered to be approximately equal to the diffraction-limited response with a 2 mm pupil $\mathrm{MTF_{DL2\,mm}}$ due to the small pupil size [13,15]. However, this approximation excludes intraocular scattering. Under these assumptions, an estimation of the eye response with a 4 mm pupil, which is here called $\widehat{\mathrm{MTF}}_{4\,\mathrm{mm}C}$, is obtained as follows:

$$\begin{aligned}\widehat{\mathrm{MTF}}_{4\,\mathrm{mm}C} &= \frac{\mathrm{MTF_{DPu}}}{\mathrm{MTF_{DL2\,mm}}}\\ &= \frac{\mathrm{MTF_{2\,mm}} \cdot \mathrm{MTF_{FS}} \cdot \mathrm{MTF_{4\,mm}}}{\mathrm{MTF_{DL2\,mm}}}\\ &\approx \mathrm{MTF_{FS}} \cdot \mathrm{MTF_{4\,mm}}.\end{aligned} \tag{2}$$

We propose to estimate the eye response with a 4 mm pupil with data processing that uses information not only from the asymmetric system, as conventionally done, but also from the symmetric DP configuration. To do this, the response $\mathrm{MTF_{DPe}}$ is used to filter the contribution of $\mathrm{MTF_{2\,mm}}$ from $\mathrm{MTF_{DPu}}$. The main advantages are that this estimation is independent of any approximation, and that undesired multiple fundus scattering effects are reduced. The proposed estimation is called $\widehat{\mathrm{MTF}}_{4\,\mathrm{mm}}$, and is computed as follows:

$$\begin{aligned}\widehat{\mathrm{MTF}}_{4\,\mathrm{mm}} &= \frac{\mathrm{MTF_{DPu}}}{\sqrt{\mathrm{MTF_{DPe}}}}\\ &= \frac{\mathrm{MTF_{2\,mm}} \cdot \mathrm{MTF_{FS}} \cdot \mathrm{MTF_{4\,mm}}}{\mathrm{MTF_{2\,mm}} \cdot \sqrt{\mathrm{MTF_{FS}}}}\\ &= \sqrt{\mathrm{MTF_{FS}}} \cdot \mathrm{MTF_{4\,mm}}.\end{aligned} \tag{3}$$

Comparing the eye responses obtained by conventional data processing and the proposed method given in Eqs. (2) and (3), respectively, we observe that the term accounting for the undesired effects of multiple fundus scattering is affected by a square root, thereby reducing the impact of $\mathrm{MTF_{FS}}$ in the latter case. Therefore, we expect estimations closer to the real eye response with a 4 mm pupil by following the proposed method. The expression in Eq. (3) is only valid at frequencies where $\mathrm{MTF_{DPe}}$ contains relevant information, that is to say, when the response for equal entrance and exit pupil diameters has such magnitude that the computation is not affected by any indetermination. In ideal systems, unaffected by aberrations or scattering, the indetermination may occur around the cutoff frequency of the system imposed by the 2 mm pupil.

The proposed method may be seen as a process to apply individualized correction curves (filters) that compensate for the decrease in magnitude of the MTF caused by undesired multiple fundus scattering of the measured eye. If this is true, the resultant curves should be independent of changes of multiple scattering with wavelength due to different penetration depths in the ocular fundus [10]. However, the verification of this statement is beyond the scope of this work. An alternative approach producing similar results is to propose a single nonlinear scaling correction curve that compensates for the expected decrease in magnitude for the majority of the population at the measured wavelength. However, it would be necessary to somehow *a priori* determine whether the proposed curve should be applied to avoid unacceptable estimation errors in particular eyes whose behavior is not well described by the average curve.

For comparison, we are also interested in obtaining an estimation of the asymmetric DP response, but with reduced contribution of undesired multiple scattering. This estimation is called the $\widehat{\mathrm{MTF}}_{\mathrm{DPuR}}$ and will be used later to quantify the effects of multiple fundus scattering taking as reference the measured response $\mathrm{MTF_{DPu}}$. To obtain this, we approximate the first-pass response with a 2 mm pupil by the one predicted by diffraction. Then, this known response is convolved (multiplied) with the estimation of the MTF for a 4 mm pupil obtained before given by Eq. (3). Thus,

$$\begin{aligned}\widehat{\mathrm{MTF}}_{\mathrm{DPuR}} &= \mathrm{MTF_{DL2\,mm}} \cdot \widehat{\mathrm{MTF}}_{4\,\mathrm{mm}}\\ &= \mathrm{MTF_{DL2\,mm}} \cdot \sqrt{\mathrm{MTF_{FS}}} \cdot \mathrm{MTF_{4\,mm}}.\end{aligned} \tag{4}$$

The asymmetric DP response here differs from the one in Eq. (1) in the sense that blurring by multiple scattering effects has been reduced by a square root of the original contribution. In addition, the estimation does not contain any intraocular scattering effects that may be affecting $\mathrm{MTF_{2\,mm}}$ in the measured response $\mathrm{MTF_{DPu}}$.

The contribution of multiple fundus scattering may be not only reduced, but also suppressed when intraocular scattering is negligible. In this situation, the assumption that $\mathrm{MTF_{2\,mm}}$ tends towards $\mathrm{MTF_{DL2\,mm}}$ is more justified than in previous cases, where intraocular scattering may play a role, and the square root of $\mathrm{MTF_{FS}}$ can be approximated as

$$\sqrt{\mathrm{MTF_{FS}}} \approx \frac{\sqrt{\mathrm{MTF_{DPe}}}}{\mathrm{MTF_{DL2\,mm}}}. \tag{5}$$

When Eq. (5) is valid, an estimation of the eye response with a 4 mm pupil with suppressed fundus scattering effects may be obtained. To do this, the remaining fundus scattering effects that are still present in the estimation $\widehat{\mathrm{MTF}}_{4\,\mathrm{mm}}$ may be suppressed by dividing Eq. (3) with the term $\sqrt{\mathrm{MTF_{FS}}}$ from

Eq. (5). For comparison purposes, this procedure is also applied to the estimation of the asymmetric DP response with reduced fundus scattering effects $\widehat{\mathrm{MTF}}_{\mathrm{DPuR}}$ in Eq. (4). In this case, the estimation with suppressed undesired fundus scattering effects may be computed as follows:

$$\widehat{\mathrm{MTF}}_{\mathrm{DPuS}} = \frac{\widehat{\mathrm{MTF}}_{\mathrm{DPuR}}}{\sqrt{\mathrm{MTF}_{\mathrm{FS}}}} = \mathrm{MTF}_{\mathrm{DL2\,mm}} \cdot \mathrm{MTF}_{4\,\mathrm{mm}}. \quad \textbf{(6)}$$

Finally, the expressions in this section have been presented considering only the magnitude of the DP responses in the Fourier domain. However, the method may also be applicable with phase by making use of optical transfer functions (OTFs).

B. Apparatus

A system that incorporates two DP configurations and an HS sensor was used during experimentation. This modified version of the instrument described in Ref. [16] is shown in Fig. 1. The system is able to perform simultaneous DP measurements with equal [1,14] and unequal [13] entrance and exit pupil diameters while the subject looks at an external object in an open-field configuration. A single entrance pupil with 2 mm diameter is used in both configurations. The pair of captured DP images is set by exit pupils of 2 and 4 mm, respectively.

Collimated light from a superluminescent diode SLD with a peak emission at 801 nm wavelength and a spectral width of 37 nm reaches the entrance pupil P_1. Compared to visible light, stronger multiple scattering effects are expected due to the increased penetration of infrared light [10]. However, its lower visibility makes measurements more comfortable for the subjects. The pupil P_1 is located at the object plane of the telescopic system $L_1 - L_2$, which imposes a magnification of $m = -1$ by using two achromatic lenses with 200 mm focal length in a $4f$ configuration. The beam is transmitted through the linear polarizer B_1 and reflected by the beam splitter BS_1 before it reaches the first lens of the telescope. Then, it is reflected by the beam splitter BS_2 and the prism mirror M_1 towards the lenses L_2 and L_T, respectively. The latter lens corresponds to a tunable device that is located at the image plane of the telescope. L_T is used in combination with the compensating lens L_C to correct spherical refractive errors at the pupil plane [17] of up to ± 6 D. The prism mirror M_2 is used to redirect light within the optical path of the corrector. The dichroic mirror DM reflects light towards the hot mirror HM at the working wavelength and allows the camera CM_P to monitor the position of the eye and the pupil size. Experimental measurements of the incident power indicate that the eye is exposed to 0.78 μW during the measurements, which is well within the safety limits [18].

The light backscattered by the ocular fundus follows an optical path similar to that described above until reaching the beam splitter BS_2. That redirects the light towards the DP cameras and the HS sensor, respectively. The light traverses L_1 and BS_1 before reaching the cube beam splitter BS_3. Two circular apertures, P_2 and P_3, act as exit pupils for the DP configurations with equal and unequal entrance and exit pupils. These apertures are located at the image plane of the telescope $L_2 - L_1$ in front of the cameras CM_{DP1} and CM_{DP2}. The recording devices capture DP images with a resolution of 0.182 arcmin. On the other hand, the light transmitted by BS_2 arrives at the lens L_3 with a focal length of 100 mm, and to the linear polarizer B_2. The set of crossed polarizers B_1 and B_2 is used to diminish corneal reflections in the HS images. The lenses L_2 and L_3 form a telescope with a magnification of $m = -0.5$. The HS sensor is positioned at the image plane of the system $L_2 - L_3$, and consist of the microlens array L_{HS} followed by the camera CM_{HS}. The lenslet array of the HS sensor has pitch and a focal length of 200 μm and 6.3 mm, respectively. The HS camera captures images with a pixel resolution of 5.3 μm.

The instrument is controlled via a graphical user interface (GUI) programmed in MATLAB (MathWorks, 2010). For instance, real-time video from the pupil, the DP, and the HS cameras is available in the GUI. The optical power of the spherical refractive error corrector can be both manually and automatically set up through a series of available tools.

As a preliminary step before experimentation, the best possible second-pass responses of the two DP configurations available in the instruments were measured. To do this, a pair of images was captured with the DP cameras CM_{DP1} and CM_{DP2} while the apparatus was illuminated with collimated light at the position of the eye. These images, denoted as I_{2P1} and I_{2P2}, represent the best possible system responses for the 2 and 4 mm pupils and are used during the application of the method to reduce the blurring of multiple fundus scattering effects. The details of the computations are explained in Section 2.E.

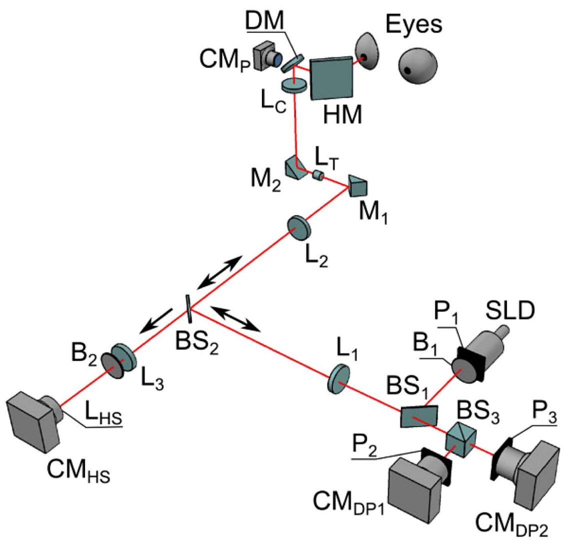

Fig. 1. Schematic representation of the DP system used during the measurements. The meaning of the labels is explained in the text.

C. Subjects

The system presented above was used to measure an artificial eye and 19 healthy right eyes of volunteers from 21 to 38 years of age with clear ocular media. The artificial eye consisted of an achromatic doublet lens with a focal length of 50 mm followed by a cardboard representing the ocular fundus. On average, the subjects were 27.68 ± 4.97 years old; 15 of them had dark-brown eyes and four had blue- or green-colored eyes. The subjects were informed about the study, and their consent was obtained. The study followed the tenets of the Declaration of Helsinki.

D. Experimental Procedure

The task of each subject consisted in looking in normal visual conditions onto a fixation target located at a distance of 6 m. First, the spherical refractive error of the eye under assessment was measured and corrected. This task was performed in less than 1 s, and made use of six HS images to estimate the optical power that was configured in the corrector available in the instrument. Afterwards, six images per DP and HS camera were recorded using an integration time of 120 ms, with an overall duration of around 1 s. In this case, a set of background images was recorded with the subjects removed from the system and a light trap was placed in the pupil plane. During the session, the alignment of the eye with the instrument was constantly monitored during the image acquisition; if the alignment was not correct, a blink was detected, or a pupil smaller than 4 mm was noticed, the recordings were discarded and the process was repeated until obtaining a valid set of images.

E. Data Processing

The six recordings per camera were averaged to obtain DP and HS images less affected by speckle. The bias of the cameras and the influence of internal reflections and possible artifacts were eliminated by subtracting the corresponding average background image. Cropped versions of the DP images of 256 × 256 pixels in size were Fourier-transformed and normalized to their values at 0 cyc/deg to obtain the responses of the equal and unequal configurations in the frequency domain. The magnitudes of such responses are, respectively, denoted as $\mathrm{MTF}_{\mathrm{DPe}}$ and $\mathrm{MTF}_{\mathrm{DPu}}$.

In order to keep parameters from the measured DP image as a reference, the method to reduce and suppress unwanted multiple fundus scattering effects was analyzed using estimations of unequal DP responses. The reduced and suppressed versions were obtained by computing $\widehat{\mathrm{MTF}}_{\mathrm{DPuR}}$ and $\widehat{\mathrm{MTF}}_{\mathrm{DPuS}}$ using Eqs. (4) and (6), respectively. The diffraction-limited responses with 2 ($\mathrm{MTF}_{\mathrm{DL2\,mm}}$) and 4 mm ($\mathrm{MTF}_{\mathrm{DL4\,mm}}$) pupils were estimated as the magnitude of the Fourier transforms of the images I_{2P1} and I_{2P2}, respectively, captured before the experimentation stage. These estimations were then used to estimate the best possible DP response with the unequal configuration as $\mathrm{MTF}_{\mathrm{DPuDL}} = \mathrm{MTF}_{\mathrm{DL2\,mm}} \cdot \mathrm{MTF}_{\mathrm{DL4\,mm}}$.

Two-dimensional DP images with a reduced contribution of multiple fundus scattering were obtained to visualize the effects of the method in the spatial domain. For this purpose, unequal DP responses $\widehat{\mathrm{MTF}}_{\mathrm{DPuR}}$ were obtained following Eq. (4), but including the phase during the calculations. The DP images were then computed by applying an inverse Fourier transform to these estimations.

The DP MTF curves that are presented in this work represent one-dimension versions of the surfaces $\widehat{\mathrm{MTF}}_{\mathrm{DPuR}}$, $\widehat{\mathrm{MTF}}_{\mathrm{DPuS}}$, and $\mathrm{MTF}_{\mathrm{DPuDL}}$ introduced above. They were obtained by computing their radial profiles, and extrapolating the zero frequency [13] from a curve fitting based on a combination of two exponential functions [19].

A relative Strehl ratio was used as an estimator of the optical quality of the assessed eye. It was computed as the ratio between the area under the DP MTF curves and that obtained with the best possible case $\mathrm{MTF}_{\mathrm{DPuDL}}$. Regarding HS data, the wave aberrations were estimated using 54 Zernike coefficients with a 4 mm pupil. The root-mean-square (RMS) error was used as a global indicator of aberrations in the measured eye.

3. RESULTS AND DISCUSSION

A. Artificial Eye

Figure 2 shows the DP response of the artificial eye with unequal pupil diameters $\mathrm{MTF}_{\mathrm{DPu}}$ and the corresponding estimations $\widehat{\mathrm{MTF}}_{\mathrm{DPuR}}$ and $\widehat{\mathrm{MTF}}_{\mathrm{DPuS}}$ with reduced and suppressed scattering from the cardboard used in the retinal plane. Compared to the measured response, the estimations presented higher magnitudes at all spatial frequencies with relevant information. In addition, the estimation with suppressed scattering overlapped with the best possible DP response of the system $\mathrm{MTF}_{\mathrm{DPuDL}}$. The curves $\mathrm{MTF}_{\mathrm{DPu}}$, $\widehat{\mathrm{MTF}}_{\mathrm{DPuR}}$, and $\widehat{\mathrm{MTF}}_{\mathrm{DPuS}}$ presented relative Strehl ratios of 0.66, 0.81, and 0.99, respectively. These values indicate a proportional improvement in the optical quality when the methods for reduction and suppression of scattering from the ocular fundus are applied.

The artificial eye was composed of an achromatic doublet lens followed by a cardboard acting as a simplistic ocular fundus. In this configuration, the system is essentially without astigmatism, higher-order aberrations, and intraocular scattering. Considering that defocus was corrected during the measurements, the deviations between the measured and expected curves $\mathrm{MTF}_{\mathrm{DPu}}$ and $\mathrm{MTF}_{\mathrm{DPuDL}}$ are only attributed to the effects of the cardboard. Quantified with the three-dimensional profiler PLu apex (Sensofar) [20], the cardboard presented height fluctuations of 3.98 μm. The characteristics of this material are obviously not accurately representative of the ocular fundus of a human eye. More complex retinal models are being developed but are beyond the scope of the present work [21,22]. However, the deviations in the unequal DP response that are attributed to the cardboard were reduced in the estimation $\widehat{\mathrm{MTF}}_{\mathrm{DPuR}}$

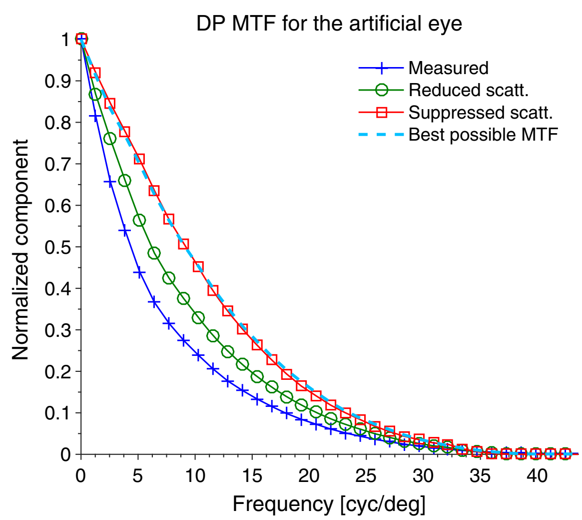

Fig. 2. Measured DP MTF of the artificial eye for unequal pupil diameters (line with plus signs). The best possible unequal DP response (discontinuous line), and the estimated curves with reduced (line with circles) and suppressed (line with squares) scattering are also plotted.

and successfully suppressed in $\widehat{\mathrm{MTF}}_{\mathrm{DPuS}}$. The latter case is corroborated by an overlap between the estimation with suppressed multiple fundus scattering and the best possible response, and therefore by a relative Strehl ratio close to unity.

B. Human Eyes

Cropped versions (10×10 arcmin) of three measured DP images for unequal pupil diameters are shown in Fig. 3 together with their corresponding estimations with reduced scattering. Visual inspection of the images indicates a strong correlation in terms of shape between the measured and the estimated responses. However, the surroundings of the DP spot appear to be more defined after the application of the method to reduce the effects of the multiple fundus scattering. For example, the characteristic pattern in the DP response labeled as S1 is also noticed in the estimation, but with a modified version of the veil surrounding the central part of the spot.

The method to reduce and suppress fundus scattering effects in the human eyes was analyzed using MTF curves plotted in Fig. 4. As for the artificial eye, the average curves indicate a proportional increment in the MTF after applying the method to reduce the impact of multiple scattering. The relative Strehl ratio of the average response increased from 0.46 in the measured response to 0.52 and 0.63 in the estimations.

The individual values of the Strehl ratio of the measured eyes and the corresponding estimations can be seen in Fig. 5 as a function of the RMS error of the Zernike coefficients measured with the HS aberrometer. The tendency lines are included in the figure to visualize the behavior of the three data sets. While the Strehl ratio is an indicator of the optical quality in the DP image, the RMS error is a metric that summarizes the wavefront aberrations of the eye. As expected, there is an inversely proportional relationship between these two parameters. The tendency lines fitting the data have similar slopes, but different y interceptions. This indicates that the estimations with reduced and suppressed fundus scattering effects are a shifted version of measured data when the Strehl ratio is considered.

Figure 5 suggests that the dispersion of the Strehl ratios around the tendency line observed in the measured data decreased in the estimation with reduced scattering. This is corroborated by the determination coefficient (r^2) of the model described by the tendency line, which varied from 0.70 to 0.90. These values indicate a higher correspondence between the relative Strehl ratio (SR) computed from DP images and the RMS error of the Zernike coefficients after applying the method to reduce the effects of scattering. There are different factors that may produce deviations between the DP and HS data, for example, the contribution of higher-order aberrations to the former technique. However, the RMS error was computed using 54 Zernike coefficients, and the measurements

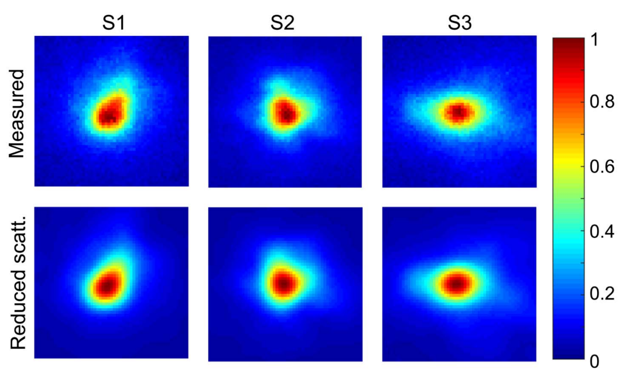

Fig. 3. Measured DP images for unequal pupil diameters (top) and their correspondent estimations with reduced impact of multiple scattering from the ocular fundus (bottom).

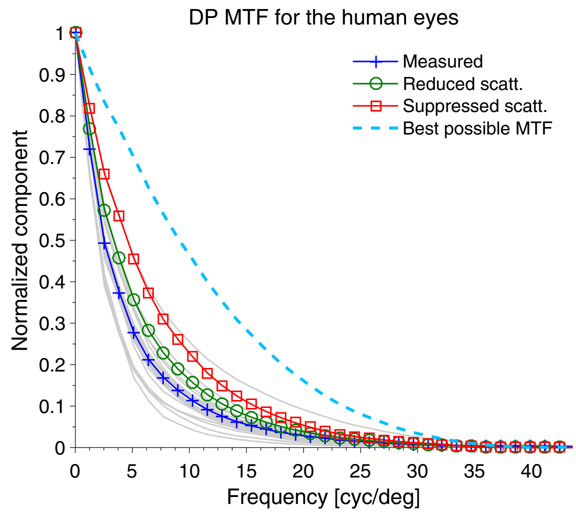

Fig. 4. Individual (lines in light gray) and average (line with plus signs) asymmetric DP MTF for the human eyes. The best possible DP response (discontinuous line), and the estimated average curves with reduced (line with circles) and suppressed (line with squares) scattering are also plotted.

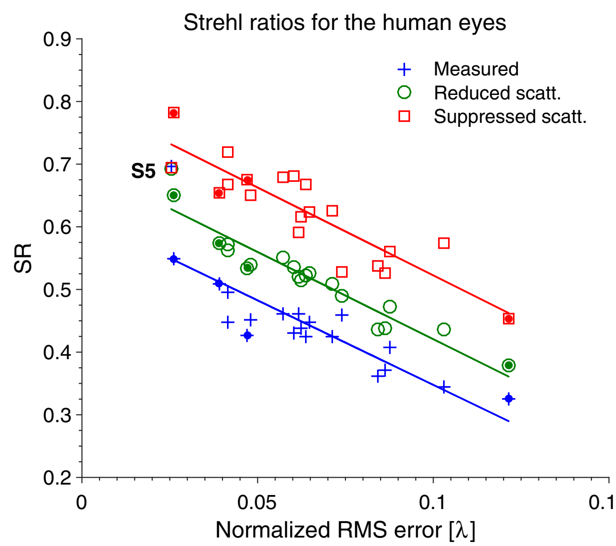

Fig. 5. Relative Strehl ratios of the measured (plus signs) and the estimated responses with reduced (circles) and suppressed (squares) scattering as a function of the RMS error computed from HS data. Information for colored eyes are indicated with a point at the center of the markers. The tendency lines fitting the data are also included (continuous lines). The overlapped Strehl ratios of subject labeled as S5 are indicated in the figure.

were performed in subjects with a maximum age of 38 years with no visual problems. Assuming that the computed wave aberrations are representative of the measured eye, and that axial and transversal alignment errors were properly corrected by the operator during measurements, we believe that the main factor influencing the deviations between the DP and HS data was differences in the ocular fundus of the participants. The increase of the determination coefficient of the tendency line in the estimation with reduced scattering indicates that the influence of the ocular fundus may be decreased with the method that has been proposed in this work.

The determination coefficient of the estimation with suppressed scattering was 0.78, a lower value than observed in the estimations with reduced scattering. The suppression of fundus scattering effects is only valid when the contribution of both intraocular scattering and aberrations is negligible in the DP images for the configuration with equal pupil diameters. In some cases, these characteristics may not be true. For instance, the oldest of the participants could plausibly be affected by larger amounts of intraocular scattering [23]. Although the images were obtained using a pupil of 2 mm, the curves used to estimate the effects of multiple scattering may present some deviations with respect to one predicted by diffraction due to uncorrected astigmatism or the presence of higher-order aberrations that could be quantified as multiple scattering effects. Based on this information, the dispersion of the Strehl ratios with suppressed scattering and the corresponding tendency line may be attributable to invalidations of the method to compensate completely for the undesired effects of the ocular fundus due to deviation of $MTF_{2\,mm}$ with respect to $MTF_{DL2\,mm}$.

The estimations are, in general, a shifted version of the measured data. However, not all the cases followed this behavior. As observed for the data of subject S5 in Fig. 5, the measured and the two estimated curves presented Strehl ratios of around 0.7. This measurement corresponds to a 23-year-old subject with dark-brown eyes. It was the only case where the overlap between computed values was noticed. This indicates that the method to reduce and suppress multiple fundus scattering effects did not cause significant changes in the resulting MTF curves. Due to this particular behavior, the alternative approach mentioned in Section 2.A of using a single nonlinear correction curve that compensates for multiple fundus scattering effects for the majority of the population would have failed to provide a representative MTF of subject S5.

The measured response and the estimation with reduced scattering presented a very strong correlation in terms of Strehl ratios (Pearson correlation coefficient $r = 0.931$, $p < 0.0001$). A mean and standard deviation (SD) of 0.075 ± 0.028 were found for the differences between the estimation and the measured response. The range between the 95% confidence limits (CLs) was 0.112 for this case. Regarding the estimation with suppressed scattering, it presented a moderate correlation with the measured data ($r = 0.640$, $p < 0.0030$), with a mean and SD of 0.176 ± 0.067 for the differences between the estimated and measured response, and a CL range of 0.262. The corresponding Bland–Altman plots can be seen in Fig. 6.

The mean of the differences between the measured and the estimated responses quantifies the gradual increment that the SR experimented. For instance, the statistics of the measured

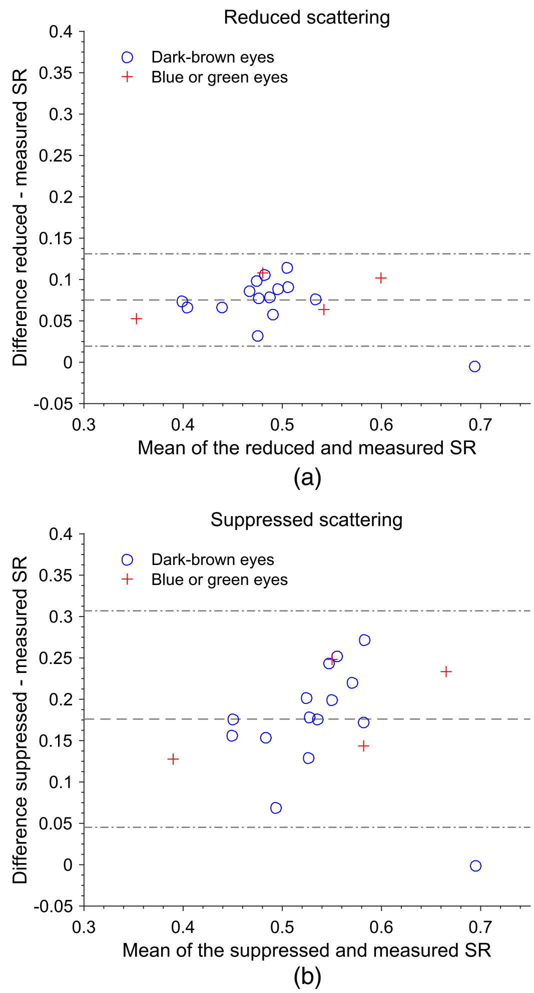

Fig. 6. Bland–Altman plots representing the differences between the estimated and measured SR as a function of the mean of such data for the (a) reduced and (b) suppressed scattering cases. The discontinuous lines show the mean of the differences and the corresponding 95%. The data for dark-brown (circles) and colored eyes (plus signs) are presented in the figure.

data indicates that estimations with reduced scattering degradation may be obtained by shifting the SR by 0.075 or 0.112, respectively. The use of shifting (correction) factors may work for the majority of the cases to provide more accurate SR values. In the reduced scattering case, the SD and CL range are close to 0.022 and lower than 0.129, values found by Vilaseca *et al.* [24] for intrasubject and intrasession repeatability using a commercial DP instrument. Regarding the suppressed case, intraocular scattering and uncorrected aberrations may be the main causes of the moderate correlation that the estimation presented with respect to the measured response. On the other hand, brown eyes (dark) and green and blue eyes (light) followed a similar tendency.

4. CONCLUSIONS

A method to reduce the impact of multiple fundus scattering in DP estimations has been presented. The procedure consists in deconvolving from the measured response with unequal entrance and exit pupil diameters the contribution of the first pass using information from a second configuration with equal entrance and exit pupil diameters. Measurements of an artificial eye corroborated that the effects of the material used as an ocular fundus were not only reduced, but also suppressed after applying the proposed method.

The measurements in real eyes indicated that DP estimations may be underestimated under the presence of fundus scattering. A mean increment in the Strehl ratio of 0.075 and 0.112 was found after applying the method to reduce and suppress fundus scattering effects. This behavior was not a rule for all the eyes, and depends on the characteristics of the measured ocular fundus. For instance, measurements of a young dark eye presented no differences after reducing the effects of the ocular fundus. Based on the results, part of the deviation between DP and HS data may come from the scattering that arises in the fundus.

The estimations with reduced scattering effects presented a very strong correlation with the measured data. The differences between the SR computed from the estimation and the measured data presented a dispersion that is comparable to the repeatability observed in systems currently used in clinical practice [24].

Funding. Horizon 2020 Framework Programme (H2020) (TECNIOspring PLUS) (712949); Agència per la Competitivitat de l'Empresa (ACCIÓ).

REFERENCES

1. J. Santamaría, P. Artal, and J. Bescós, "Determination of the point-spread function of human eyes using a hybrid optical-digital method," J. Opt. Soc. Am. A **4**, 1109–1114 (1987).
2. B. Vohnsen, "Directional sensitivity of the retina: a layered scattering model of outer-segment photoreceptor pigments," Biomed. Opt. Express **5**, 1569–1587 (2014).
3. F. C. Delori and K. P. Pflibsen, "Spectral reflectance of the human ocular fundus," Appl. Opt. **28**, 1061–1077 (1989).
4. J. van de Kraats, T. T. Berendschot, and D. van Norren, "The pathways of light measured in fundus reflectometry," Vision Res. **36**, 2229–2247 (1996).
5. I. J. Hodgkinson, P. B. Greer, and A. C. B. Molteno, "Point-spread function for light scattered in the human ocular fundus," J. Opt. Soc. Am. A **11**, 479–486 (1994).
6. D. R. Williams, D. H. Brainard, M. J. McMahon, and R. Navarro, "Double-pass and interferometric measures of the optical quality of the eye," J. Opt. Soc. Am. A **11**, 3123–3135 (1994).
7. D. Christaras, H. Ginis, and P. Artal, "Spatial properties of fundus reflectance and red-green relative spectral sensitivity," J. Opt. Soc. Am. A **32**, 1723–1728 (2015).
8. H. S. Ginis, G. M. Perez, J. M. Bueno, A. Pennos, and P. Artal, "Wavelength dependence of the ocular straylight," Invest. Ophthalmol. Visual Sci. **54**, 3702 (2013).
9. D. Christaras, H. Ginis, A. Pennos, and P. Artal, "Scattering contribution to the double-pass PSF using Monte Carlo simulations," Ophthalmic Physiolog. Opt. **37**, 342–346 (2017).
10. N. López-Gil and P. Artal, "Comparison of double-pass estimates of the retinal-image quality obtained with green and near-infrared light," J. Opt. Soc. Am. A **14**, 961–971 (1997).
11. J. Liang and D. R. Williams, "Aberrations and retinal image quality of the normal human eye," J. Opt. Soc. Am. A **14**, 2873–2883 (1997).
12. C. E. García-Guerra, M. Aldaba, M. Arjona, F. Díaz-Doutón, J. A. Martínez-Roda, and J. Pujol, "Response for light scattered in the ocular fundus from double-pass and Hartmann–Shack estimations," J. Opt. Soc. Am. A **33**, 2150–2157 (2016).
13. P. Artal, D. G. Green, I. Iglesias, and N. López-Gil, "Double-pass measurements of the retinal-image quality with unequal entrance and exit pupil sizes and the reversibility of the eye's optical system," J. Opt. Soc. Am. A **12**, 2358–2366 (1995).
14. P. Artal, S. Marcos, D. R. Williams, and R. Navarro, "Odd aberrations and double-pass measurements of retinal image quality," J. Opt. Soc. Am. A **12**, 195–201 (1995).
15. F. W. Campbell and R. W. Gubisch, "Optical quality of the human eye," J. Physiol. **186**, 558–578 (1966).
16. C. E. García-Guerra, M. Aldaba, M. Arjona, and J. Pujol, "Binocular open-view system to perform estimations of aberrations and scattering in the human eye," Appl. Opt. **54**, 9504–9508 (2015).
17. F. Sanàbria, F. Díaz-Doutón, M. Aldaba, and J. Pujol, "Spherical refractive correction with an electro-optical liquid lens in a double-pass system," J. Eur. Opt. Soc. **8**, 13062 (2013).
18. I. E. Commission, "Safety of laser products-Part 1: Equipment classification and requirements," Test Report IEC 60825-1, 2014.
19. P. Artal and R. Navarro, "Monochromatic modulation transfer function of the human eye for different pupil diameters: an analytical expression," J. Opt. Soc. Am. A **11**, 246–249 (1994).
20. A. Pintó, F. Laguarta, R. Artigas, and C. Cadavall, "Non-contact measurement of aspherical and freeform optics with a new confocal tracking profiler," Proc. SPIE **8169**, 81690V (2011).
21. D. Valente and B. Vohnsen, "Retina-simulating phantom produced by photolithography," Opt. Lett. **42**, 4623–4626 (2017).
22. N. Kedia, Z. Liu, R. Sochol, D. X. Hammer, and A. Agrawal, "3D printed phantoms of retinal photoreceptor cells for evaluating adaptive optics imaging modalities," Proc. SPIE **10474**, 104740D (2018).
23. J. A. Martínez-Roda, M. Vilaseca, J. C. Ondategui, M. Aguirre, and J. Pujol, "Effects of aging on optical quality and visual function," Clin. Exp. Optom. **99**, 518–525 (2016).
24. M. Vilaseca, E. Peris, J. Pujol, R. M. Borrás, and M. Arjona, "Intra- and intersession repeatability of a double-pass instrument," Optom. Vision Sci. **87**, 675–681 (2010).